Elyns Publishing Group
Explore and Exploit

www.elynsgroup.com

Research Article Journal of Biomedical Technology and Research Open Access

A Testing Platform to Evaluate Thermal Profiles of Balloon Catheter-based Bipolar Radiofrequency Ablation Devices in the Treatment of Resistant Hypertension

Laura K Hobbs[1], Lori Shaw-Klein[2], William J Grande[2], Greg T Gdowski[1]*

[1]University of Rochester, Center for Medical Technology & Innovation, Department of Biomedical Engineering, 218 Goergen Hall, Box 270168, Rochester, NY, 14647-0168 USA.
[2]Micropen Technologies Corporation, 93 Paper Mill Street, Honeoye Falls, New York 14472.

Abstract

Radiofrequency (RF) ablation is currently being developed for renal denervation, a medical procedure used to treat resistant hypertension. This treatment involves the local heating of tissue surrounding the renal artery to a temperature sufficient for nerve ablation without causing irreversible damage to arterial tissue. One of the greatest difficulties in improving the effectiveness of this technology is in determining how thermal energy spatially dissipates throughout the tissue during the procedure. This is dependent not only on the properties of the tissue, but on the size, location, and material properties of the RF stimulating electrodes. We developed a testing platform that utilizes a novel additive manufacturing process developed by Micropen Technologies Corporation for printing RF ablation electrodes on polyethylene terephthalate (PET) medical balloons. Micropen's technology allowed us to customize balloon prototypes having arrays of RF stimulating electrodes. Longitudinal and circumferential RF stimulation array patterns were produced so that the thermal distribution within porcine renal arterial tissue, which offered the best anatomical representation of human renal arterial tissue, could be assayed with a single thermocouple placed within the tissue. The different array patterns allowed us to determine the spatial thermal profile at the site of RF ablation in two dimensions including along the long axis of the balloon and around its circumference. The testing platform allows for the precise measurement of RF ablation temperature profiles so that future devices can be optimized in terms of the stimulating array configuration and the material properties of stimulating electrodes.

Introduction

One of the leading causes of heart attack, heart disease, and stroke is hypertension, a disease characterized by a chronic elevated blood pressure level above 140/90 mmHg [1]. According to the Center for Disease, Control and Prevention, as many as 1 in every 3 American adults, or nearly 67 million individuals, has been diagnosed with hypertension [2]. There are many causes of hypertension, both external such as a diet high in sodium and internal such as increased sodium reabsorption, increased renal sympathetic nerve activity and hyperactivation of the renin-angiotensin-aldosterone system [3]. The renin-angiotensin-aldosterone system is a hormone regulatory system controlled by signals from the kidneys to the pituitary gland and vice versa [3]. Given that the cause of hypertension in some patients is the over-activity of this regulatory system, many patients may continue to display chronic hypertension even when antihypertensive medications are used in parallel with lifestyle adjustments [4]. In fact, nearly 8.9% of individuals have been classified as resistant hypertensive, characterized by a blood pressure greater than or equal to 140/90 mm Hg that could not be lowered by using antihypertensive medications from three different drug classes or drugs from four or more antihypertensive drug classes [3,5]. All of these individuals are considered to have an increased risk of cardiovascular events [6].

In the 2009 Simplicity HTN-2 trial, it was shown that a disruption of the neural innervation of the kidney resulted in a significant drop in blood pressure (32/12 mmHg) in agroup of 49 patients with resistant hypertension [7]. These results suggested that renal denervation could be used as a therapeutic surgical procedure as an alternative to ineffective pharmaceutical therapies. The procedure was done by first placing an electrode-tipped catheter through the femoral artery and advancing it into the renal artery in close proximity to the kidneys [7]. Radio frequency (RF) energy was then delivered through the electrodes of the catheter to produce an increase in thermal energy within the arterial wall that resulted in a persistent disruption of renal nerve activity. The majority (84%) of subjects who underwent renal denervation had a persistent reduction in systolic blood pressure of 10 mm Hg or more for six months following the procedure [7]. Renal function was assessed six months post-procedure by quantifying serum creatinine, eGFR, and cystatin C concentrations, concluding that these metrics remained unchanged from baseline in both the control and renal denervation group [7]. These results suggested that renal denervation could be safely used to substantially reduce blood pressure in treatment-resistant hypertensive patients, which has inspired several companies to develop renal denervation devices [8-11].

In September of 2013, Medtronic's Symplicity system for renal denervation announced the first randomized, blinded, and sham controlled trial in 1,000 U.S. patients [12]. Although the system achieved its primary safety endpoint, more importantly it was reported to have failed to meet the primary efficacy endpoint. This occurred partially because a reduction in systolic blood pressure was observed in the sham group and there was also significant variability in the reduction observed among the control group. This led to Medtronic to question whether renal denervation therapy was effective compared with its control and they subsequently withdrew early from their clinical trials [13]. Despite this outcome, Medtronic remains optimistic about the future of renal denervation and states that further research is warranted to identify and mitigate the underlying reasons for failure [12,13]. One reason for the failure to reach efficacy could be related to the device not being fully apposing the arterial wall in all subjects. Nonetheless, Medtronic's withdrawal from the trial was unexpected within the medical device industry because of the promising results that were reported in previous trials [7,14]. These studies place further emphasis on the need to develop a method of standardizing the testing of these devices prior to beginning clinical trials, thereby ensuring that the devices are delivering sufficient power to the tissue to adequately ablate the renal nerves.

The renal nerves consist of afferent and efferent nerve fibers travelling to and from the kidney that participate in the regulation of different aspects of cardiac function [14]. Stimulation of the afferent renal nerves results in increasing heart rate and consequentially increases the oxygen consumption of the heart [15]. On the other hand, the efferent renal nerves function to sympathetically stimulate the release of the hormone renin that helps in the reabsorption of sodium by reducing blood flow through the kidney [15]. This results in an increase in the volume of fluid circulating in the body due to the retention of salt and water by the kidneys, causing higher blood pressure. Since there is no direct correlation between heart rate and blood pressure, the main targets of RF ablation for alleviating hypertension are thought to be overactive efferent renal nerves [16,17]. In a 2012 study of renal denervation performed on 15 patients with stage 3-4 chronic kidney disease (CKD), it was found that the bilateral renal denervation procedure reduced systolic blood pressure by about 30 mmHg, but the in-office and ambulatory heart rate measurements did not significantly change after renal denervation was performed [14]. The systolic blood pressures of the patients were monitored at 1, 3, 6, and 12 months after the procedure and systolic blood pressure remained reduced, suggesting that the renal nerves had been adequately ablated [14]. In agreement with Medtronic's findings that renal denervation presents no significant safety risk to patients, this study also concluded that there was no significant alterations in kidney function, which was quantified by a measurement of glomerular filtration rate (GFR) [14]. Additionally, the serum and urine biochemistry displayed no statistically significant differences post-procedure [14].

A recent anatomical study showed that renal nerves course throughout all layers of the renal artery, half of which are concentrated within 0.5 to 1.0 mm of the arterial wall adjacent to the lumen of the vessel [18]. The results suggest that nearly half of the innervation of the kidney by the renal nerve could be ablated if thermal changes produced by RF energy could be limited to regions in close proximity to the lumen wall. Even more importantly, it suggests that successful clinical outcomes may be achievable without adversely damaging the tissue and causing arterial stenosis or necrosis that compromises the vessel's integrity for carrying blood to the kidneys. Consequently, there is a great need for the development of a testing system to provide quantification of this procedure. Such a testing platform would ultimately guide the engineering of catheter-based RF stimulating electrodes to produce targeted spatial patterns of thermal changes within and along the arterial wall for ablating renal nerve activity.

The Department of Biomedical Engineering at the University of Rochester partnered together with Micropen Technologies (Honeoye Falls, NY) to develop a testing platform for catheter-based RF ablation. The platform was developed as part of a senior design project in Biomedical Engineering, which was continued as an ongoing partnership with the Center for Medical Technology & Innovation at the University of Rochester. Micropen Technologies specializes in printing conductive inks onto medical devices including balloon catheters that are commonly used for vascular procedures. Their technology was used to print arrays of electrodes onto balloon catheters in longitudinal and circumferential patterns so that RF energy could be delivered to precise locations along the inside lumen of an excised porcine renal artery. A porcine model for the renal artery was chosen because it offered the greatest similarities to the human renal artery anatomy in diameter and branching from only a single renal artery per kidney [19]. A thermocouple was placed within the renal artery segment to quantify the spatial distribution of thermal changes induced by RF energy. The results demonstrate a testing platform that can be used to guide the development of RF stimulating electrode arrays to produce optimal thermal patterns for ablating nerve activity within the renal artery for the purposes of treating resistant hypertension.

Methods

Medical Balloon Device

A 5mm diameter, 40 mm long polyethylene terephthalate (PET) medical balloon (Vention Medical, model 05004023CA) was used to test the RF platform. Two configurations of spatially arranged arrays of stimulating electrodes/pads were printed onto the surface of the balloon wall (Micropen Technologies Corporation, Honeoye Falls, NY). Each stimulating electrode was printed using polymeric silver ink as a rectangular pad having dimensions of 1.02 mm by 4.06 mm. An individual silver ink trace (width 1 mm) was printed longitudinally along the length of the medical balloon to each of the stimulating electrodes. An insulating layer of chlorinated polyolefin was printed over the entire length of the silver trace up to the RF stimulating electrode pads, which were left exposed. Insulated wires were then connected to each of the silver wires at the distal end of the medical balloon so that the thermal tests could be carried out while submerged in a water bath. Figure 1 shows the two different electrode array configurations that were tested. The first configuration (Figure 1a) consisted of eight RF stimulating electrodes that were arranged longitudinally along the medical balloon that were placed 1.27 mm apart, center to center, with a separation of 0.25 mm between the edges of two adjacent electrodes. The second configuration (Figure 1b) consisted of eight RF stimulating electrodes that were arranged around the circumference of the medical balloon with the same physical spacing along the arc length of the balloon.

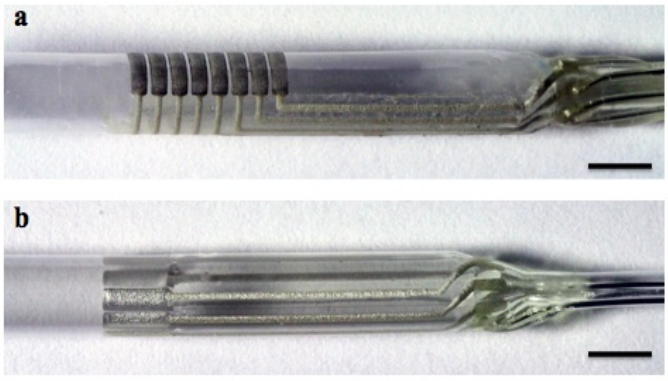

Figure: 1

Figure 1 (a) **Balloon devices with eight conductive polymeric silver ink RF pads (1.02 mm by 4.06 mm) and insulated silver ink traces, applied by Micropen Technologies, in (a) a longitudinal array and (b) a circumferential array. PET balloons are 5 mm x 40 mm (Vention Medical, model 05004023CA). Scale bars: 4 mm**

The medical balloon was modified so that it could be easily inflated and deflated. A Becton Dickinson (BD)Insyte™ Autoguard™ shielded IV catheter was attached to one end of the balloon with silicone, while the other end of the balloon was sealed with silicone. The inflation level was manipulated with a syringe filled with saline that was connected to the IV catheter.

RF delivery and data acquisition

RF power (1W) at 400 kHz was delivered with a commercially available RF electrosurgical unit (model Sabre 2400,ConMed Corporation, Utica, NY). Two adjacent RF stimulation electrodes were used to produce bipolar RF stimulation where one electrode served as the active and the other as the ground. A multimeter (GDM8245; GW Instek) was placed in series with the RF surgical unit to verify RF delivery to the RF stimulating electrodes. A low-drift,type K, transition junction thermocouple probe was used to make temperature measurements (Omega KMTSS-032G-6). The sensitivity of this thermocouple was40 μV/°C and it had atime constant of 0.23 seconds in water, a probe diameter of 0.80 mm, and an upper limit of 371°C.The selection of this probe permitted temperature measurements to be made in small confined areas proximal to the probe's tip. A thermocouple amplifier with cold junction temperature compensation (Analog Devices AD8495) was constructed (Gain=120) so that analog records of temperature could be digitized. The output of the thermocouple amplifier was low-pass filtered to reduce noise while recording data during experiments. Temperature was digitized using a National Instruments Educational Laboratory Virtual Instrument Suite (ELVIS) that had an analog to digital converter that was used to digitize temperature at a sampling rate of 100 Hz. Custom software and graphical user interfaces were developed within Lab view for calibrating and acquiring temperature data during experiments.

Testing Platform

The testing platform was designed to accurately assess changes in temperature produced across the renal artery during RF ablation, while controlling and maintaining the temperature of the external environment with a water bath regulated to 37°C. To accomplish this, renal arteries were blunt dissected from porcine kidneys that were acquired from a slaughterhouse. The renal artery was completely extracted from the surrounding adipose and connective tissue so that temperature could be recorded directly adjacent to the vessel's exterior wall. The diameter of the renal arteries was approximately 5mm.

The balloon device was placed into the renal artery segment by deflating the balloon so that it could be inserted into the lumen. Once inserted, it was inflated with saline at 37°C in order to situate the RF stimulating electrodes adjacent to the inside arterial wall. Porcine adipose tissue (approximately 5 mm in thickness) was then replaced around the artery to approximate the tissue removed during the vessel extraction process.

The thermocouple was placed directly on the outside wall of the artery using a stereotactic positioner (David Kopf Instruments) through a small, 1mm diameter hole that was dissected into the adipose tissue.

The tissue, balloon device, and thermocouple were then submerged in the water bath. This process functioned to isolate the tip of the thermocouple probe from the water bath and to restrict temperature measurements to the outside surface of the artery. The position of the entire system and thermocouple was not changed or modified throughout the experiments. Thermal properties produced by activating RF stimulating electrodes were quantified by manipulating only the pattern of stimulation to the array of electrodes.

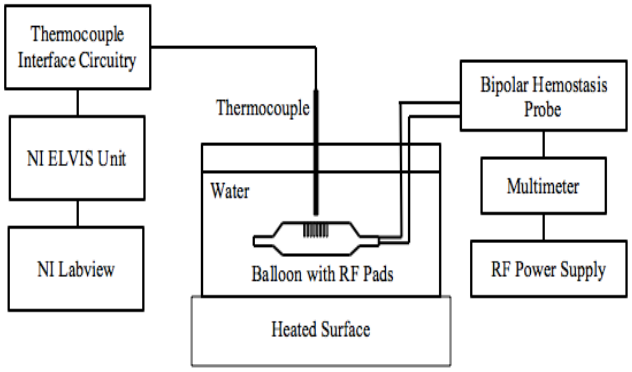

Figure: 2(a)

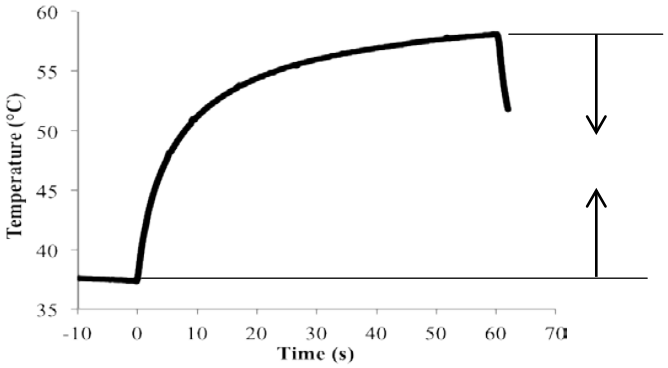

Figure: 2(b)

Figure 2(a) Schematic of the experimental setup used for experiments. The adipose tissue and arterial tissue layers around the balloon are omitted in this diagram and the thermocouple location could be adjusted by a three way positioner to be between pads 1 and 2 or between pads 4 and 5 depending on the type of experiment performed. Water bath temperature was maintained at 37 °C± 2 °C for all experiments. (b) Characteristic temperature of a 60 second ablation experiment. The RF power is turned on at 10 seconds and turned off at 70 seconds and the temperature is measured on surface of the artery. This heating region can be modeled with a power function.

Temperature Measurement

The thermocouple was positioned using a stereotactic positioner (David Kopf Instruments) against the outer arterial wall between two RF stimulating electrodes of the array. For the symmetry experiments, the fourth and fifth electrode pads were stimulated, as shown in Figures 3a and 4a. For the length constant experiments, the first and second electrode pads were stimulated, as shown in Figures 5a and 6a, allowing for measurements to be made at a farther distance from the thermocouple. The thermocouple remained stationary through the duration of the experiment and then pairs of electrodes were sequentially stimulated.

Change in temperature was calculated as the difference in temperature between 0 seconds and 60 seconds of RF ablations (Figure 2b). The temperature of the water bath was kept at 37 ± 2°C. The distance from the center of the two electrodes carrying the current to the thermocouple probe was used to yield a temperature profile across the surface of the balloon. Each pad was tested a total of three times for each experiment, allowing for the calculation of an average temperature rise at each distance and this procedure was repeated on five different days for each type of experiment. Statistical analysis of each experiment included all fifteen trials from that experiment.

The average longitudinal and circumferential length constant data was used to determine the coordinate at which a certain temperature change was reached (e.g. 10 °C). The coordinates for each temperature were used to fit an ellipse representing the thermal profile of that value in MATLAB (v.7.13.0). This was used to model a 3-D surface contour plot of heat radiating from the RF pad region.

Length Constant Determinatio

A length constant was determined for the longitudinal and circumferential RF patterns to give an indication of the distance required to dissipate heat from the electrode. The thermocouple was placed between the first two electrodes and each pair of electrodes along the array was stimulated, allowing for data at a farther distance from the RF pad (Figure 5a, 6a). Each pad was tested a total of three times for each experiment, allowing for the calculation of an average temperature rise at each distance. Five days of experiments for both the longitudinal and circumferential balloons' statistical analysis included all fifteen trials. Data from each experiment was plotted as change in temperature versus distance away from stimulation, and fit to a decaying exponential in MATLAB (v7.13.0). The length constant was calculated by taking the negative inverse of the exponential constant of the fit.

Data Analysis

Custom software written in MATLAB (v7.13.0) was used to analyze temperature data acquired during RF stimulation. Algorithms for carrying out least-squared exponential fits were used to quantify the spatial constants for thermal dissipation along the arterial wall. Statistical differences between the mean ΔTvalues at each distance for the longitudinal and circumferential symmetry experiments were evaluated using 1-way ANOVA in Prism 6. Tukey post-hoc analysis in Prism 6 was used to determine significance between ΔT values at each distance.

Results

Longitudinal Symmetry Experiment

The mean temperature change at the RF pad for the longitudinal thermal symmetry experiment was 20.9± 1.4 °C after 60 seconds of ablation. This duration of ablation was chosen because it was the time at which the recorded temperature reached target temperature for nerve ablation. Statistical analysis via 1-way ANOVA showed a significant difference between mean temperature change for at least one distance ($p<0.001$). A Tukey post-hoc analysis revealed that the mean temperature rise directly at the heating RF pad was significantly different than the mean temperature rise at any other location ($p<0.05$). Additionally, the mean temperature rise at a location some distance from the heating RF pad was not significantly different than the mean temperature rise at the same distance in the other direction, suggesting a symmetrical distribution of heating ($p<0.05$).

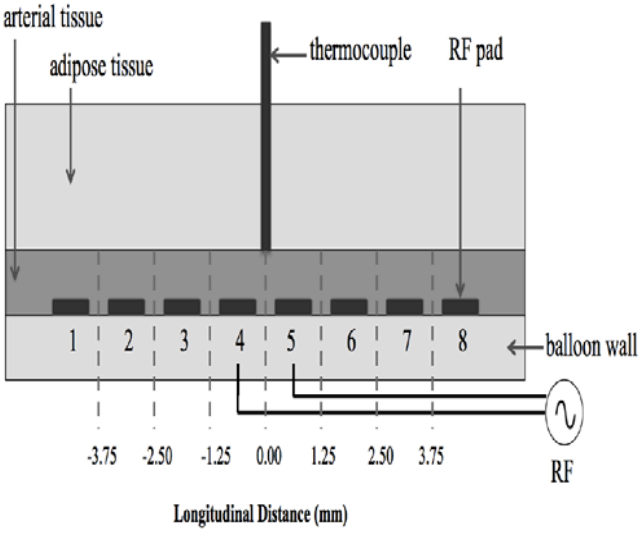

Figure: 3(a)

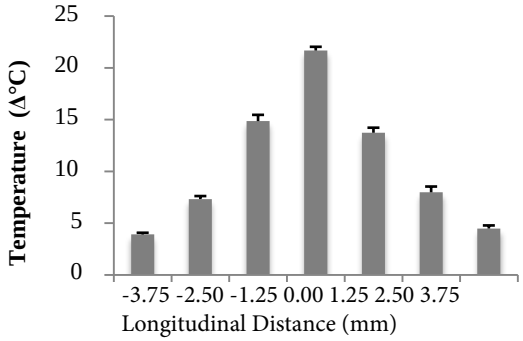

Figure: 3(b)

Figure 3(a) Diagram of the longitudinal symmetry experiment setup, with the thermocouple positioned on the surface of the arterial tissue located between pads 4 and 5. Shown are the balloon wall (20µm thickness), arterial tissue (0.63 ± 0.05mm thickness and 4.91 ± 0.19mm diameter), and adipose tissue (4.94

± 0.07mm thickness). Not drawn to scale (b) Thermal longitudinal symmetry experiment, n=5. Data represents average change in temperature at each distance for the longitudinal balloon. Error bars represent s.e.m. (n=5).

Circumferential Symmetry Experiment

The mean temperature change at the RF pad for the circumferential thermal symmetry experiment was 21.7± 0.4 ºC after 60 seconds of ablation. Statistical analysis via 1-way ANOVA showed a significant difference between means ($p<0.001$). Tukey post-hoc analysis revealed that the mean temperature rise directly at the heating RF pad was significantly different than the mean temperature rise at any other location ($p<0.05$). Additionally, the mean temperature rise at a location some distance from the heating RF pad was not significantly different than the mean temperature rise at the same distance in the other direction, suggesting a symmetrical distribution of heating ($p<0.05$).

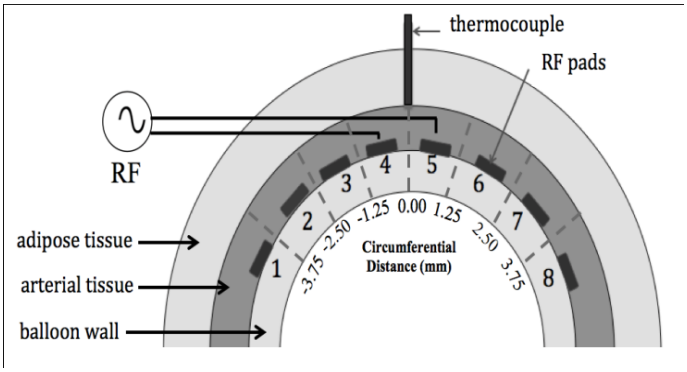

Figure: 4(a)

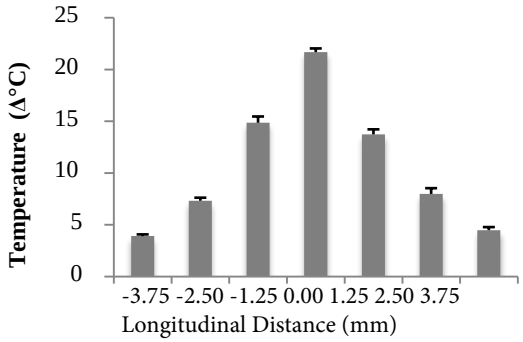

Figure: 4(b)

Figure 4 (a) Diagram of the setup when performing a circumferential symmetry experiment, where distance is measured as arc length. The thermocouple is positioned on the surface of the arterial tissue, between pads 4 and 5. Shown are the balloon wall (20µm thickness), arterial tissue (0.56 ± 0.03mm thickness and 5.00 ± 0.03mm diameter), and adipose tissue (5.02 ± 0.09mm thickness). Not drawn to scale. (b) Thermal circumferential symmetry experiment, n=5. Data represents the average change in temperature at each distance for the circumferential balloon. Error bars represent s.e.m. (n=5).

Longitudinal Length Constant

The mean temperature change at the RF pad for the longitudinal thermal length constant experiment was 22.7± 0.4 ºC after 60 seconds of ablation. The decaying exponential fit had a R2 value of 0.995 with an average length constant of 2.7 mm. The 90% confidence interval for the circumferential length constant was calculated to be [2.6, 2.8] mm (n=5). Figure 5b gives the longitudinal characteristic length constant profile and exponential regression for the thermal dissipation along the length of the artery.

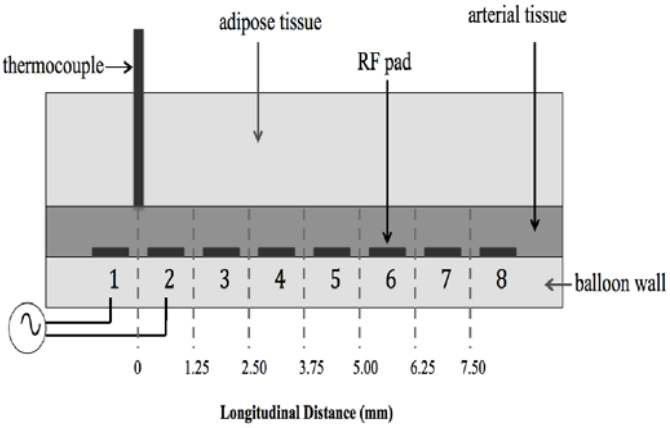

Figure: 5(a)

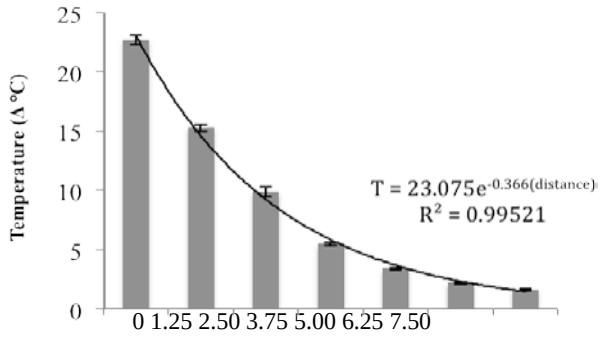

Figure: 5(b)

Figure 5 (a) Diagram of setup for the longitudinal length constant experiments. Thermocouple is placed on the surface of the artery between the first and second RF pad. Shown are the balloon wall (20µm thickness), arterial tissue (0.52 ± 0.03mm thickness and 4.67 ± 0.21mm diameter), and adipose tissue (4.64 ± 0.25mm thickness). Not drawn to scale (b) Longitudinal length constant data, n=5. Data represents the average change in temperature at each longitudinal distance. Data was fitted to a decaying exponential, with the average fit displayed. Error bars represent s.e.m (n=5).

Circumferential Length Constant

The mean temperature change at the RF pad for the circumferential thermal length constant experiment was 21.0± 0.2 °C after 60 seconds of ablation. The decaying exponential fit had a R2 value of 0.968 with an average circumferential length constant of 2.1 mm. The 90% confidence interval for the circumferential length constant was calculated to be [2.0, 2.3] mm (n=5). Figure 6bgives the characteristic length constant profile and exponential regression for the thermal dissipation along the circumference of the artery.

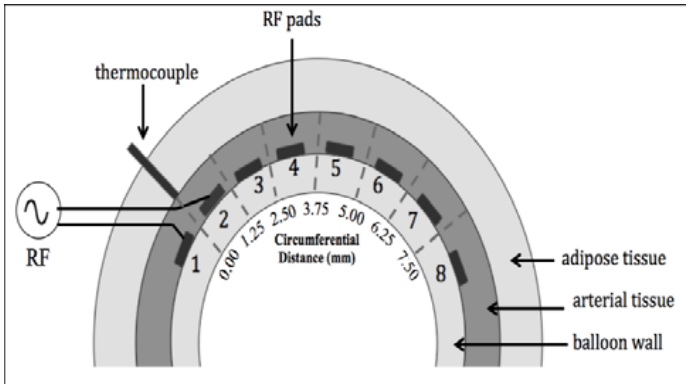

Figure: 6(a)

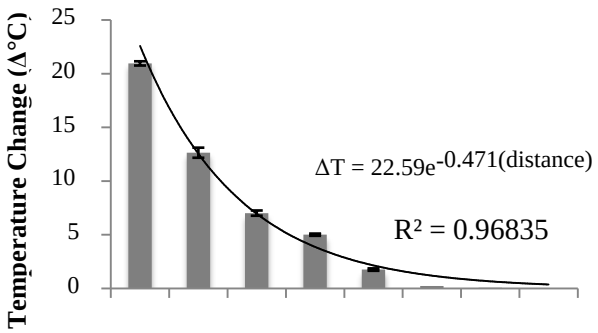

Figure: 6(b)

Figure 6 (a) Diagram of setup for the circumferential length constant experiments. Thermocouple is placed on the surface of the artery between the first and second RF pad. Shown are the balloon wall (20 µm thickness), arterial tissue (0.50 ± 0.03 mm thickness and 5.10 ± 0.1 mm diameter), and adipose tissue (4.87 ± 0.12 mm thickness). Not drawn to scale (b) Circumferential length constant data, n=5. Data represents the average circumferential heating at each distance from the thermocouple. Data was fitted to a decaying exponential, with the average fit displayed. The farthest two data points were omitted from this fit, as the temperature change was so small. Error bars represent s.e.m (n=5).

Surface Contour Plot

Figure 7a shows a surface contour plot of heating from an RF pad with Figure 7b showing the corresponding heating contours. This model utilizes the average longitudinal and circumferential length constant exponential decay fits to determine the coordinates at which a certain temperature was reached. These coordinates were fit to an ellipse and this process was repeated for a number of different temperature change values. These ellipses were modeled in MATLAB (v7.13.0), shown in Figure 4a and 4b.

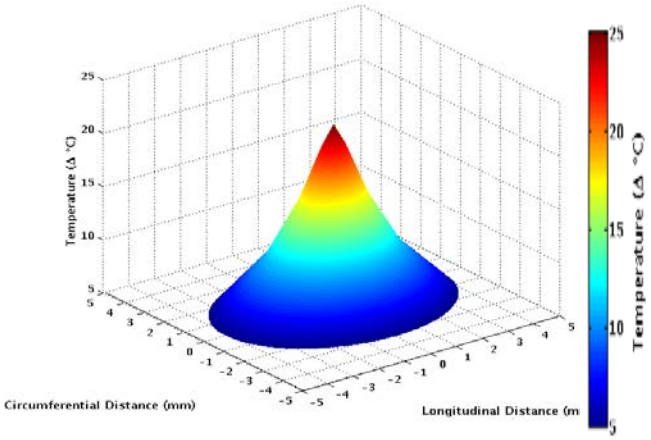

Figure: 7(a)

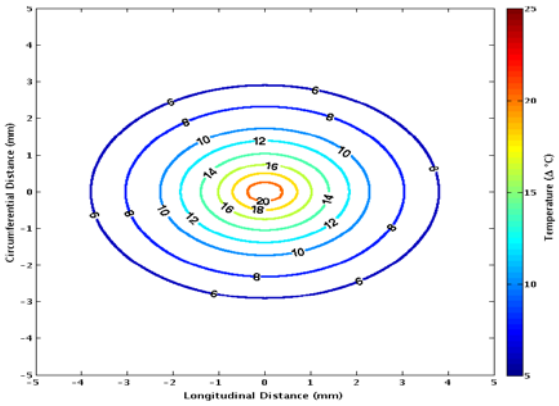

Figure: 7(b)

Figure7 (a) Surface contour plot showing the dissipation of heat around the RF pad being stimulated. Average longitudinal and circumferential length constant data was used to determine the coordinate at which a certain temperature change was reached (e.g. 10 °C). The coordinates for each temperature were used to fit an ellipse representing the thermal of that value. (b) 3-D surface plot of dissipation of heat around the RF pad being stimulated. Each ellipse from (a) was plotted and this surface plot was generated in MATLAB.

Discussion

An understanding of the heat dissipation resulting from bipolar RF ablation of the sympathetic nerves in the renal artery is necessary for the design and testing of new renal denervation devices. Current temperature monitoring protocols measure the temperature of the artery directly at the site of ablation [8-11]. The goal of our work was to expand upon these singular point measurements by creating a testing platform capable of determining how far heat dissipates around the area of ablation and thus allowing for the optimization of an RF ablation electrode pattern while improving safety and efficacy of the renal denervation procedure. The longitudinal and circumferential temperatures were evaluated as well as length constants for each direction.

This work demonstrates that bipolar RF ablation of renal sympathetic nerves at 1W results in a temperature distribution along the length and circumference of the artery. The mean temperature change at the RF pad for the longitudinal thermal symmetry experiment was 20.9± 1.4°C and the mean temperature change for the circumferential thermal symmetry experiment was 21.7± 0.4°C after 60 seconds of ablation. The maximum temperature achieved at the site of ablation was 25.3°C over 37°C, and the heating displayed an exponential decay in both longitudinal and circumferential directions. The length constant of longitudinal temperature decay was 2.7± 0.1°C and that of circumferential temperature decay was 2.1±0.1°C.

In order to simulate the anatomical variations that may occur naturally, a new artery and layer of adipose tissue was used for each ablation. Therefore, the confidence intervals reported for length constants should reflect these natural anatomical variations. It is important to note that porcine renal arteries have an approximate wall thickness of 1 mm, whereas human renal arteries have an average wall thickness of 2.5 mm [14]. Future work could be directed at studying the difference in heat dissipation resulting from artery wall thickness, changes in heat dissipation with increasing power, or producing a setup that more accurately reflects the human renal artery anatomy.

Of the devices currently designed for renal denervation, there is no consensus on what parameters are most appropriate for effective ablation of renal sympathetic nerves. Power level, target temperature, and duration of ablation vary considerably among devices [8-11]. The thermal data reported in this paper, combined with data from clinical trials of renal denervation devices, help further the development of a standard for renal denervation parameters.

Acknowledgements

We wish to thank all individuals that contributed to initial design and testing of the system including: Joshua Holtzberg, James Jeng, Ian Marozas, Natalie Mitchel and John Nicosia. The authors would also like to thank the Center for Emerging & Innovative Sciences at the University of Rochester for their financial support offered through the STAR program.

Competing Interests Statement

The authors declare that they have no competing interests.

*Corresponding Author: Greg Gdowski, Ph.D, Executive Director University of Rochester, Center for Medical Technology & Innovation, Department of Biomedical Engineering, 218 Goergen Hall, Box 270168, Rochester, NY 14647-0168 USA, Tel: (585) 275-2580; Fax: (585) 276-1999; E-mail: Greg_Gdowski@urmc.rochester.edu.

Received Date: April 21, 2014, **Accepted Date: June** 2, 2014, **Published Date:** June 5, 2014.

Citation: Laura K Hobbs, Lori Shaw-Klein, William J Grande, Greg T Gdowski (2014) A Testing Platform to Evaluate Thermal Profiles of Balloon Catheter-based Bipolar Radiofrequency Ablation Devices in the Treatment of Resistant Hypertension. J Biom Tech Res 1(1): 8.

References

1. Logan AG, Perlikowski SM, Mente A, Tisler A, Tkacova R, et al. (2001) High prevalence of unrecognized sleep apnoeain drug-resistant hypertension. J Hypertens 19: 2271-2277.

2. Centers for Disease Control and Prevention (2012) Vital signs: awareness and treatment of uncontrolled hypertension among adults -- United States, 2003-2010. MMWR. Morbidity and mortality weekly report 61: 703-709.

3. Khawaja Z, Wilcox CS (2011) Role of the kidneys in resistant hypertension. Int J Hypertens 143471.

4. Calhoun DA, Textor S, Goff DC, Murphy TP, Toto RD, et al. (2008) Resistant hypertension: diagnosis, evaluation, and treatment; a scientific statement from the American Heart Association Professional Education Committee of the Council for High Blood Pressure Research. Circulation 51: 1403-1419.

5. Persell SD (2011) Prevalence of Resistant Hypertension in the United States, 2003-2008. Hypertension 57: 1076-1080.

6. Steinberger JD, Daniels SR (2003) Obesity, insulin resistance, diabetes, and cardiovascular risk in children, an American Heart Association scientific statement from the Atherosclerosis, Hypertension, and Obesity in the Young Committee (Council on Cardiovascular Disease in the Young) and the Diabetes Committee (Council on Nutrition, Physical Activity, and Metabolism). Circulation 107: 1448-1453.

7. Esler MD, Krum H, Sobotka PA, Schlaich MP, Schmieder RE, et al. (2010) Renal sympathetic denervation in patients with treatment-resistant hypertension (The Symplicity HTN-2 Trial): a randomised controlled trial. Lancet 376: 1903-1909.

8. Templin C, Jaguszewski M, Ghadri JR, Sudano I, Gaehwiler R, et. al (2013) Vascular lesions induced by renal nerve ablation as assessed by optical coherence tomography: pre- and post-procedural comparison with the Simplicity® catheter system and the EnligHTN™ multi-electrode renal denervation catheter. Eur Heart J 34: 2141-2148.

9. Ormiston JA, Watson T, van Pelt N, Stewart R, Haworth P, et al. (2013) First-in-human use of the OneShot™ renal denervation system from Covidien. EuroIntervention 8: 1090-1094.

10. Krum H, Barman N, Schlaich M, Sobotka P, Esler M, et al. (2012) Long-term follow-up of catheter-based renal denervation for resistant hypertension confirms durable blood pressure reduction. Journal of the American College of Cardiology 59: 1704.

11. Mahfoud F, Lüscher TF, Andersson B, Baumgartner I, Cifkova R, et al. (2013) Expert consensus document from the European Society of Cardiology on catheter-based renal denervation. Eur Heart J 34: 2149-2157.

12. Medtronic Global SYMPLICITY registry shows strong safety profile of the Symplicity™ renal denervation system (2014) Medtronic Inc.

13. Medtronic Announces U.S. Renal Denervation Pivotal Trials Fails to Meet Primary Efficacy Endpoint While Meeting Primary Safety Endpoint (2014) Med Device Online.

14. Hering D, Mahfoud F, Walton AS, Krum H, Lambert GW, et. al. (2012). Renal denervation in moderate to severe CKD. J Am Soc Nephrol 23: 1250-1257.

15. Kopp UC (2011) Neural control of renal function, Colloquium Series on Integrated Systems Physiology: From Molecule to Function. Morgan & Claypool Life Sciences 3: 1 96.

16. Thames MD, DiBona GF (1979) Renal nerves modulate the secretion of rennin mediated by nonneural mechanisms. Circulation research 44: 645-652.

17. Reule S, Drawz PE (2012) Heart rate and blood pressure: any possible implications for management of hypertension? Curr Hypertens Rep 14: 478-484.

18. Atherton DS, Deep NL, Mendelsohn FO (2012) Micro-anatomy of the renal sympathetic nervous system: A human postmortem histologic study. Clin Anat 25: 628-633.

19. Pereira-Sampaio MA, Favorito LA, Sampaio FJ (2004) Pig kidney: anatomical relationships between the intrarenal arteries and the kidney collecting system. Applied study for the urological research and surgical training. J Urol 172: 2077-2081.